Volume Representation of Parenchymatous Organs by Volumetric Self-organizing Deformable Model

Shoko Miyauchi[1(✉)], Ken'ichi Morooka[1], Tokuo Tsuji[2], Yasushi Miyagi[3], Takaichi Fukuda[4], and Ryo Kurazume[1]

[1] Kyushu University, Fukuoka, Japan
miyauchi@irvs.ait.kyushu-u.ac.jp
[2] Kanazawa University, Ishikawa, Japan
[3] Fukuoka Mirai Hospital, Fukuoka, Japan
[4] Kumamoto University, Kumamoto, Japan

Abstract. This paper proposes a new method for describing parenchymatous organs by the set of volumetric primitives with simple shapes. The proposed method is based on our modified Self-organizing Deformable Model (mSDM) which maps an object surface model onto a target surface with no foldovers. By extending mSDM to apply to organ volume models, the proposed method, volumetric SDM (vSDM), finds the one-to-one correspondence between the volume model and its target volume. During the mapping, vSDM preserves geometrical properties of the original model while mapping internal structures of the model onto their corresponding primitives inside of the target volume. Owing to these characteristics, vSDM enables to obtain a new volume representation of organ volume models which simultaneously (1) represents by simple primitives the shapes of the whole organ and its internal structures and (2) describes the relationship among the external surface and internal structures of the organ.

1 Introduction

Human body contains many parenchymatous organs which have internal structures and/or blood vessels within the external surface of the organ. Recent medical imaging devices provide high-resolution volume models of the parenchymatous organs. The volume model of a human organ in our method consists of a set of tetrahedra. The organ volume models are useful for many medical applications including statistical analysis of target organs in individuals and surgical simulators. Here, human organs such as brain surfaces have complicated shape. Moreover, the volume model of the parenchymatous organ consists of a huge number of points. For these reasons, the processes using directly the volume models are time-consuming. Therefore, the description of the organ volume model is important for the medical applications to deal with the organ volume models efficiently.

M. Reuter et al. (Eds.): SeSAMI 2016, LNCS 10126, pp. 39–50, 2016.
DOI: 10.1007/978-3-319-51237-2_4

In the case of the surface models of human organs, one approach for this problem is to represent the organ surface on a common simple surface (referred to as a target surface) such as a plane or a spherical surface by mapping these organs onto the target surface [4,12]. This makes it possible to easily compare among the organs and analyze them via the target surface.

In the case of the organ volume model, in order to understand the structural features of the parenchymatous organ, the model description method needs to represent not only the shapes of the whole organ and its internal structures but also the spatial relations between the external surface and internal structures of the organ. When the conventional mapping methods for the surface model is applied to the volume models, the organ volume is represented as the set of the surface models of the organ and its internal structures. However, this volume model description meets the first requirement, but not the second one.

In this paper, we propose a method for representing the volume model of a human organ with one volumetric primitive with simple shape. The proposed method is based on our modified Self-organizing Deformable Model (mSDM) [6,7]. Unlike the conventional methods for surface model mapping, mSDM enables to map an organ surface model onto its target surface with various shapes while preserving the geometrical properties of the original organ model after the mapping. By extending mSDM, our proposed method, volumetric Self-organizing Deformable Model (vSDM), maps the organ volume model onto its target volume. In the mapping, the surface of the organ is fitted to that of the target volume while each internal structure of the organ is mapped onto its corresponding inner primitive within the target volume. In addition, vSDM mapping preserves geometrical properties of the original volume model such as the angles and volumes of the tetrahedra. The previous vSDM proposed in [8,9] controls the mapping of only one internal structure to its inner primitive whose location is determined manually and fixed during the mapping. Our new vSDM introduces two new techniques: the simultaneous mapping of multi internal structures and the automatic determination of the inner primitive positions based on the structure of each volume model. Owing to these characteristics of the vSDM mapping, the volume model obtained by the vSDM mapping represents the whole organ and its internal structures by their corresponding primitives with simple shapes while describing the spatial relationship between them.

There are several mapping methods for the volume models [3,5]. Li et al. [5] developed a harmonic volumetric mapping for object volume models. The harmonic mapping preserves the length ratio among three edges forming a patch, but not the scale of the patch. vSDM can preserve both the two geometrical properties, that is, the distance along edges between any two vertices. This means that the mapped model by the vSDM describes the spatial relationship among the vertices more faithfully compared with the harmonic volumetric mapping [5]. Therefore, the use of the model obtained by the vSDM mapping enables to find a more reliable correspondence between the volume models. Hu et al. [3] proposed the volume-preserving mapping of a brain volume model onto a spherical volume. The method in [3] controls for moving a few feature vertices in

the volume model to their specific locations in the target volume. However, there is no guarantee that the method in [3] controls the mapping locations of many vertices on the surface of the internal structure while our vSDM can map the internal structures with many vertices onto their corresponding inner primitives. From these characteristics, the contribution of our work is that the vSDM can represent a volume model by a simple shape while preserving spatial relations among the internal structures.

2 Modified Self-organizing Deformable Model [6]

In mSDM, a triangular surface model $\mathcal{M}_s$ of a human organ is used as an initial mSDM. For each vertex $\boldsymbol{v}$ in $\mathcal{M}_s$, its 1-ring region R_v consists of the patches p containing $\boldsymbol{v}$. The closed surface of $\boldsymbol{v}$ is a part of the target surface enclosed by edges not including $\boldsymbol{v}$ in R_v. Moreover, we manually select the vertices from $\mathcal{M}_s$ as feature vertices, and their corresponding points from the target surface.

The overview of mSDM algorithm for mapping $\mathcal{M}_s$ onto the target surface is as follows. The detail of the algorithm can be seen in [6,7].

[m1] Deform the model $\mathcal{M}_s$ to fit to the target surface by the original SDM algorithm [10]. SDM is a deformable model based on competitive learning and energy minimization approaches. Given an organ model as the initial SDM, the model is deformed to fit to its target surface while moving several specific vertices of the model toward their corresponding points on the target surface. The SDM-based mapping is applicable to objects with various shapes as the initial SDM and the target surface although conventional mapping methods use as the target surfaces only a plane or a spherical surface.
Practically, when from the target surface, one point is randomly chosen as a control point, the vertex of $\mathcal{M}_s$ closest to the control point is used as the winner vertex. Here, when the corresponding point of the feature vertex is the control point, the feature vertex is always chosen as the winner vertex. The winner vertex and its neighbor vertices are moved toward the control point. These processes are repeated until all vertices of $\mathcal{M}_s$ are not moved.

[m2] Remove foldovers in the mapped model. This process is derived from the concept in Athanasiadis et al. [1] that if the deformed model $\mathcal{M}_s$ after step.m1 includes the vertices existing out of their closed surfaces, consider that the foldovers on the surface of $\mathcal{M}_s$ occur around the vertices. Based on the concept, we correct the foldovers by repeatedly moving all vertices in $\mathcal{M}_s$ toward the inside of their closed surface:

$$\boldsymbol{v} = \varphi\Big(\frac{\sum_{p\in R_v} A_p \boldsymbol{g}_p}{\sum_{p\in R_v} A_p}\Big), \tag{1}$$

where A_p and $\boldsymbol{g}_p$ are the area and centroid of the patch p. The function $\varphi(\boldsymbol{v})$ projects the vertex $\boldsymbol{v}$ onto the target surface. If the process is applied only to folded patches, their neighbor patches may become degenerate.

In order to avoid this situation, the process of removing foldovers is applied to all vertices and is repeated until all foldovers are removed.

[m3] If the feature vertices are far from their corresponding points, using Free-Form Deformation (FFD) [11], move each feature vertex to the location of its corresponding point by deforming the region around the feature vertex. When a lattice space is generated around the deformation region, FFD deforms an object with no foldovers by setting properly the lattice for the deformation. Practically, in our experiment, there is no foldover in all the models deformed by our FFD-based movement of the landmarks. Even though the deformed model by FFD includes some foldovers, the foldovers are removed by our foldover removal processing while fixing the landmark positions.

[m4] Deform the model $\mathcal{M}_s$ to preserve the geometrical properties of the original organ surface model after the mapping. In mSDM, We focus on the areas and angles of patches in $\mathcal{M}_s$ as the geometrical features to be preserved. The geometrical feature preserving mapping ϕ is found by minimizing an objective function E_s which is a weighted linear combination of an angle error term $E^{(R)}_{angle}$ and an area error term E_{area}:

$$E_s(\mathcal{M}_s, \phi) = \sum_{\boldsymbol{v} \in \mathcal{M}_s} [(1 - \mu_s)\psi_s E^{(R)}_{angle} + \mu_s E_{area}]; \tag{2}$$

$$E^{(R)}_{angle}(\boldsymbol{v}, \phi) = \sum_{p \in R_v} \sum_{d=1}^{3} e_{angle}(\theta^d_p, \phi); \tag{3}$$

$$E_{area}(\boldsymbol{v}, \phi) = \sum_{p \in R_v} e_{area}(p, \phi); \tag{4}$$

$$e_{angle}(\theta^d_p, \phi) = |\phi(\theta^d_p) - \theta^d_p|; \tag{5}$$

$$e_{area}(\boldsymbol{v}, \phi) = \Big| \frac{\phi(A_p)}{\phi(A_w)} - \frac{A_p}{A_w} \Big|, \tag{6}$$

where ψ_s is a scaling factor to adjust the ranges of the two error terms. θ^d_p and A_p are one angle and area of the patch p included in the 1-ring region R_v of the vertex $\boldsymbol{v}$. $\phi(\theta)$ and $\phi(A)$ are the angle and area of the patch in the mapped model $\phi(\mathcal{M}_s)$. Here, A_w and $\phi(A_w)$ are the whole areas of the original model $\mathcal{M}_s$ and $\phi(\mathcal{M}_s)$.

We decided the four processing in order of decreasing the range of moving the model vertices. In the step.m1, all the vertices are moved dynamically to map the model onto the target surface roughly. The step.m2 is to move all the vertices on the target surface to remove foldovers occurred in the first step. In the step.m3, each landmark is located at its target position by moving only the neighbor vertices of the landmark within the limited space around landmarks. The step.m4 performs the geometrical feature preserving mapping by moving each vertex within its 1-ring region. From the characteristic, our strategy changing the range of moving vertices finds the suitable mapping while avoiding local minimum like Simulated Annealing.

Fig. 1. (a) The surface of the brain volume model; (b) The brain volume model cut by two virtual planes for the interior visualization; (c) The brain surface (blue), ventricle (red), caudate nuclei (yellow), putamina (green); (d) The surface of the target volume; (e) The ITS (orange) for the right and left putamina. (Color figure online)

3 Volumetric SDM

In volumetric SDM (vSDM), a tetrahedral volume model $\mathcal{M}_v$ of a human organ is used as an initial vSDM. The external surface of $\mathcal{M}_s$ is regarded as the outer model surface (OMS) of the vSDM. vSDM contains the inner volume models of the internal structures of the organ. Several internal structures to be analyzed are selected and the surfaces of the selected internal structures are used as the inner model surfaces (IMSs) of the vSDM. One example of the initial vSDM is a brain volume model (Fig. 1(a)–(c)) which consists of brain surface (the blue part in Fig. 1(c)), ventricle (the red part), caudate nuclei (the yellow part), putamina (the green part). In this paper, the brain surface is used as the OMS while we selected as the IMSs the surfaces of the right and left putamina.

The vertices in $\mathcal{M}_v$ are classified into three types. OMS and IMS vertices are the vertices on the OMS and IMSs, respectively. The rest vertices are regarded as the inner vertices. For each vertex except the OMS vertices, its 1-ball region is defined by the set of the tetrahedra containing the vertex (Fig. 3(a)).

vSDM is mapped onto a target volume represented by a set of tetrahedra. The external surface of the target volume, called the outer target surface (OTS) is the mapping destination of the OMS. The target volume includes inner targets within the OTS. Each IMS is mapped onto its corresponding inner target surface (ITS). Here, the initial vSDM is completely covered with the OTS. The example of a target volume used in our experiment is a spherical volume model (the light blue region in Fig. 1(d) and (e)) which includes two ellipsoids (the orange regions in Fig. 1(e)). In this case, the OTS and ITSs are, respectively, the spherical surface and the two spheroidal surfaces.

Two main processes comprise our vSDM-based approach to find the volume mapping Φ of the initial vSDM to the target volume (Fig. 2). The first is to map the OMS onto the OTS while moving the inner and IMS vertices to preserve the geometrical properties of the original organ model as far as possible. The geometrical properties to be preserved are the angles of the patches and the volumes of the tetrahedra in $\mathcal{M}_v$. Therefore, the preservation process is called an angle- and/or volume-preserving mapping. The first mapping processes are denoted as ϕ_{mv} in Fig. 2.

The second process is to find a mapping ϕ_m of the mapped IMS by ϕ_{mv} (the green line in Fig. 2) onto its corresponding ITS by mSDM. To perform mSDM, the model to be deformed by mSDM needs to cover the large part of the target surface. Considering this, by using the distribution of the IMS vertices, we determine the position and pose of the LT (the orange line in Fig. 2) satisfying this requirement. The mSDM obtains the mapping ϕ_m of all IMSs to their corresponding ITSs. Moreover, we perform two processes: (1) correcting the inverted tetrahedra in the vSDM and (2) performing a angle- and/or volume-preserving mapping.

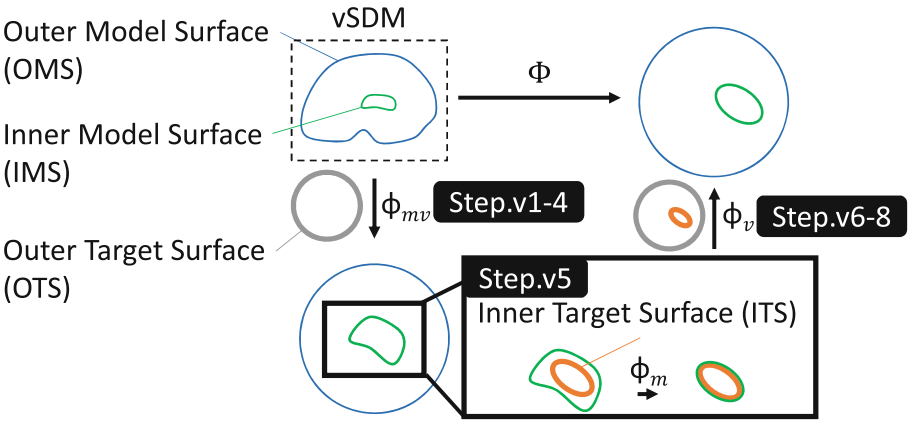

Fig. 2. Overview of vSDM. (Color figure online)

The algorithm of vSDM deformation is as follows.

[v1] Map the OMS vertices of the initial vSDM onto the OTS by step.m1, m2 and m4 of mSDM deformation.
[v2] Move each vertex except the OMS vertices toward the centroid of its polyhedron. Here, the polyhedron of a vertex $\boldsymbol{v}$ is obtained by removing from its 1-ball region the vertex $\boldsymbol{v}$ and the edges connecting with $\boldsymbol{v}$. This movement process is repeated until no vertices are moved.
[v3] Correct inverted tetrahedra by **Correction method 1**.
[v4] Perform an angle- and/or volume-preserving mapping by moving the vertices except the OMS vertices.
[v5] For each IMS,
  (i) Determine the position and pose of the corresponding LT of the IMS.
  (ii) Map the IMS vertices onto the ITS by step.m1, m2 and m4 of mSDM deformation.
[v6] Move each inner vertex toward the centroid of its polyhedron. This movement process is repeated until all inner vertices are not moved.
[v7] Correct inverted tetrahedra by **Correction method 1** and **2**.
[v8] Perform an angle- and/or volume-preserving mapping by moving only the inner vertices while fixing the OMS and IMS vertices.

Step.v1 maps only the OMS vertices onto the OTS while other vertices are distributed within the target volume in step.v2. Step.v3 corrects inverted tetrahedra in the model obtained after these steps. In step.v4, to preserve geometrical features of original model on the target volume, angle- and/or volume-preserving mapping is performed. After the positions of the IMS vertices are determined, in step.v6, the inner vertices are moved based on the positions of the OMS and IMS vertices. Finally, the algorithm performs the correction of the inverted tetrahedra (step.v7) and the angle- and/or volume-preserving mapping (step.v8).

The following describes details of the processes of correcting inverted tetrahedra (step.v3 and v7) and performing an angle- and/or volume-preserving mapping (step.v4 and v8).

3.1 Inverted Tetrahedron Correction

Depending on the shape of the polyhedron of the vertex, the vertex movement in step.v2 and v6 may lead to the self-intersections of the vSDM. As a result, the model obtained after step.v2 and v6 sometimes contains inverted tetrahedra. The inverted tetrahedra provide the wrong description of the spatial relationship among the vertices. In order to obtain the reliable description of the original volume model on the target volume, the volumetric mapping method must guarantee a one-to-one mapping with no inverted tetrahedra between the volume model and the target volume. To achieve this, in the step.v3 and v7, the inverted tetrahedra are corrected by the following two ways.

[Correction method 1]

In our method, an inverted tetrahedron is the tetrahedron whose at least one vertex exists outside the polyhedron of the vertex (Fig. 3(b)). To find the inverted tetrahedron, we use the visibility condition of the vertex from its neighbor vertices: if the vertex $\boldsymbol{v}$ is visible from all vertices of the polyhedron of $\boldsymbol{v}$, there are no inverted tetrahedra including a vertex $\boldsymbol{v}$. When we find the vertices not satisfying the condition, the tetrahedra including the vertices are regarded as to be inverted. These inverted tetrahedra are corrected by moving the vertices toward the suitable positions where the vertices meet the condition. To find such position, we check whether the polyhedron of the vertex $\boldsymbol{v}$ is a star-shaped polyhedron or not. When the polyhedron is star-shaped, the polyhedron contains the kernel region in which all points are always visible from the vertices of the polyhedron [2]. Then, the vertex $\boldsymbol{v}$ is moved to the kernel region. Otherwise, when the polyhedron of $\boldsymbol{v}$ is not star-shaped, the vertices forming the polyhedron of $\boldsymbol{v}$ are moved to their kernel region without moving $\boldsymbol{v}$.

The algorithm for correcting inverted tetrahedra is described as follows. For each vertex $\boldsymbol{v}$ except the OMS vertices, we calculate support planes (the dotted lines in Fig. 3(c)) by extending the faces of the polyhedron of the vertex $\boldsymbol{v}$. If the support planes form an enclosed region (the red region in Fig. 3(c)), the enclosed region is regarded as the kernel region of the polyhedron. Then, $\boldsymbol{v}$ is moved

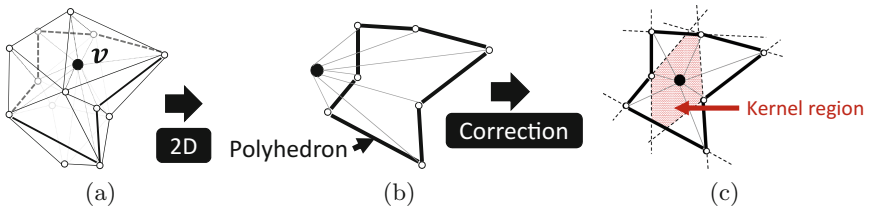

Fig. 3. Example of the inverted tetrahedron correction process shown in two dimensional space: (a) 1-ball region, (b) inverted tetrahedra, (c) normal tetrahedra. (Color figure online)

toward the centroid of the kernel region. Otherwise, the inverted tetrahedra including $\boldsymbol{v}$ are corrected by moving the vertices composing the polyhedron of $\boldsymbol{v}$ to the centroids of their kernel regions. These processes are repeated until all inverted tetrahedra are corrected.

[Correction method 2]

In the step.v7, the **Correction method 1** is applied to the inner vertices to correct the inverted tetrahedra. If after the correction, there reminds inverted tetrahedra in the vSDM, the tetrahedra are corrected by moving the IMS vertices $\boldsymbol{v}_l$ of the inverted tetrahedra along the ITS. To achieve this, by the same way as the **Correction method 1**, we check whether the kernel region of $\boldsymbol{v}_l$ exists or not. If the kernel region exists, we find the quadric surface fitted to the ITS around the kernel region of $\boldsymbol{v}_l$. When there is the overlapping area between the kernel region and the quadric surface, $\boldsymbol{v}_l$ is moved toward the centroid of the overlapping area. Otherwise, if there is neither the kernel region nor the overlapping area between the kernel region and the quadric surface, we correct the inverted tetrahedron by the **Correction method 1**. These processes of **Correction method 2** are repeated until all inverted tetrahedra are corrected.

3.2 Angle- and/or Volume-Preserving Mapping

In step.v4 and v8, the vSDM is deformed to preserve the angles of the triangle patches of a tetrahedron, and the volume of the tetrahedron. The angle- and/or volume-preserving mapping of the volume model $\mathcal{M}_v$ is to find the mapping ϕ which minimizes an objective function E_v:

$$E_v(\mathcal{M}_v, \phi) = \sum_{\boldsymbol{v} \in \mathcal{M}_v} \left[(1 - \mu_v) \psi_v E^{(B)}_{angle} + \mu_v E_{vol} \right], \tag{7}$$

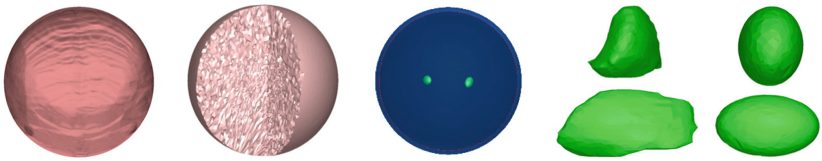

(a) (b) (c) (d) (e)

Fig. 4. (a) The final model surface with the normals of the original model; (b) The interior of the resulting model; (c) The internal organ mapped on its ITS in the final model; (d) The original left putamen from two different views; (e) The left putamen surface after vSDM deformation from the two different views.

where ψ_v is a scaling factor. The function E_v consists of a weighted linear combination of angle error distortion $E^{(B)}_{angle}$ and volume error distortion E_{vol}:

$$E^{(B)}_{angle}(\boldsymbol{v}, \phi) = \sum_{p \in B_v} \sum_{d=1}^{3} e_{angle}(\theta^d_p, \phi); \tag{8}$$

$$E_{vol}(\boldsymbol{v}, \phi) = \sum_{t \in B_v} e_{vol}(t, \phi); \tag{9}$$

$$e_{vol}(t, \phi) = \Big| \frac{\phi(V_t)}{\phi(V_w)} - \frac{V_t}{V_w} \Big|, \tag{10}$$

where θ^d_p is one angle of the patch p of the tetrahedron t containing a vertex $\boldsymbol{v}$ in $\mathcal{M}_v$. V_t and $\phi(V_t)$ are the volumes of t in the original model $\mathcal{M}_v$ and the mapped model $\phi(\mathcal{M}_v)$. V_w and $\phi(V_w)$ are the total volume of all tetrahedrons in $\mathcal{M}_v$ and $\phi(\mathcal{M}_v)$. Changing the weighting factor μ_v in Eq. (7) from 0 to 1, the mapping becomes from angle- to volume-preserving mapping.

From Eqs.(7)–(10), the minimization of the objective function E_v in Eq. (7) is replaced as the optimal location problem of the vertices within their polyhedra. A greedy algorithm is employed to find the optimal mapping which minimizes E_v. Practically, one vertex is selected randomly from all the vertices. The selected vertex is moved to a location within its 1-ball region so that E_v after moving the vertex to the location is minimized. The processes of the vertex selection and movement are repeated until all vertices are not moved.

4 Experiment

To verify the applicability of our proposed method, we made the experiment using the volume model of a brain (Fig. 1(a)–(c)). The volume model contains 153,121 vertices and 896,327 tetrahedra. From the internal structures in the brain model (Fig. 1(c)), we selected as the IMSs the right and left putamina, and denote as IMS1 and IMS2. By mapping the brain model onto the target volume with 18,246 points (Fig. 1(d) and (e)), the final mapped brain volume

model is obtained in Fig. 4. Figure 4(a) shows the brain surface mapped onto the OTS with the normals of the original model (Fig. 1(a)). Figure 4(b) shows the cross section of the final model in Fig. 4(a). Figure 4(c) shows the internal organs of the final model. Figure 4(d) and (e) show the left putamen model before and after the vSDM deformation.

We evaluate the mapping result by three criteria. First, we count the number of inverted tetrahedra in the final model. As shown in the second column of Table 1, the final mapped brain model has no inverted tetrahedra.

The second evaluation is to verify the mapping accuracy of each IMS, $\mathcal{L}$, in the final model mapped by the mapping Φ onto its ITS, $\mathcal{T}_l$. The accuracy is measured by the distance e_d between $\mathcal{L}$ and $\mathcal{T}_l$:

$$e_d(\mathcal{L}, \Phi) = \frac{1}{2}\Big(\sum_{\boldsymbol{v}_l \in \Omega_l} \frac{H(\Phi(\boldsymbol{v}_l), \mathcal{T}_l)}{|\Omega_l|} + \sum_{\boldsymbol{p}_l \in \Omega_t} \frac{H(\boldsymbol{p}_l, \Phi(\mathcal{L}))}{|\Omega_t|} \Big), \tag{11}$$

where Ω_l and Ω_t are the set of the IMS vertices $\boldsymbol{v}_l$ and the points $\boldsymbol{p}_l$ on the ITS, and $|\Omega_l|$ and $|\Omega_t|$ are the numbers of vertices in Ω_l and Ω_t, respectively. The function $H(\Phi(\boldsymbol{v}_l), \mathcal{T}_l)$ returns the Euclidean distance between the vertex $\Phi(\boldsymbol{v}_l)$ in the final model and the patch in $\mathcal{T}_l$ that is closest to $\Phi(\boldsymbol{v}_l)$. Similarly, the function $H(\boldsymbol{p}_l, \Phi(\mathcal{L}))$ returns the distance between $\boldsymbol{p}_l$ and its closest patch in $\Phi(\mathcal{L})$. The values of e_d for the mapped putamen surfaces are shown in the third and fourth columns of Table 1.

The third evaluation is to verify our angle- and/or volume-preserving mapping by using the angle error distortion e_{angle} in Eq. (5) and the volume error distortion e_{vol} in Eq. (10). In the experiment, the parameter μ_v in Eq. (7) is set to $\mu_v = 0.5$. We define the geometrical preserving ratios r_{angle} and r_{vol} as the percentages of the tetrahedra of which each geometrical error, e_{angle} and e_{vol}, is less than a given threshold. When the average angle and volume of all tetrahedra in the final mapped model are denoted as $\bar{\theta}$ and $\bar{V}$, the thresholds of e_{angle} and e_{vol} in the experiment are set to $0.3\bar{\theta}$ and $0.3\bar{V}$. The values of r_{angle} and r_{vol} before and after Step.v8 are shown in the fifth and sixth columns of Table 1, respectively.

4.1 Discussion

From Fig. 4(a)–(c) and the second column of Table 1, we can confirm that the final mapped brain model has completely the same shape of the target volume with no inverted tetrahedra. Simultaneously, the vSDM maps the right and

Table 1. The number of inverted tetrahedra (IT), e_d of IMS1 and IMS2, r_{angle} and r_{vol} before and after Step.v8.

	IT	e_d of IMS1 $[mm]$	e_d of IMS2 $[mm]$	r_{angle} [%]	r_{vol} [%]
Before step.v8	-	-	-	66.2	63.2
After step.v8	0	3.82×10^{-2}	4.27×10^{-2}	78.1	75.7

left putamina to the elliptic LT1 and LT2 (Fig. 4(d)). The mapped right and left putamina have elliptical shape (the green ellipsoids in Fig. 4(e)), and the differences e_d between the mapped putamina and their ITSs are smaller compared with LT1 and LT2 whose bounding box sizes are $32.6[mm] \times 29.8[mm] \times 53.2[mm]$ and $36.0[mm] \times 29.6[mm] \times 51.1[mm]$, respectively. This result implies that the vertices of each IMS are completely located on its ITS.

Before applying the angle- and volume-preserving mapping in Step.v8 of the vSDM deformation, r_{angle} and r_{vol} are 66.2 and 63.2 [%], respectively. After Step.v8, r_{angle} and r_{vol} increase to 78.1 and 75.7 [%]. This means performing Step.v8 improves the accuracy of preserving the geometrical properties of the original model. As mentioned above, the preservation of the two geometrical properties means that the distance along edges between any two vertices is preserved. Therefore, the final mapped model keeps the spatial relationship between the external surface and internal organs of the original model.

From these resuITS, vSDM can obtain the reliable description of the whole volume and internal structure of an organ with their corresponding simple shapes while describing the relationship among them.

5 Conclusion

In this paper, we proposed the method of representing volume models of parenchymatous organs by their target volumes. The proposed method deforms the OMS of the volume model to fit to the OTS of the target volume while moving the vertices of IMSs within the volume model onto their ITSs. Moreover, we perform two processes: correcting inverted tetrahedra and preserving the geometrical properties of the original model as far as possible. From the experimental resuITS, our method provides the volumetric description of the brain volume model composed of several internal structures which both represents the brain model by the simplified shapes of the brain surface and the internal structures, and describes the relationship among them. Our future works include the verification of the availability of our vSDM by using organ volume models with more complex structures.

Acknowledgment. This work was supported by Grant-in-Aid for JSPS Research Fellow 16J03878 and JSPS KAKENHI 16K00243.

References

1. Athanasiadis, T., Fudos, I., Nikou, C., Stamati, V.: Feature-based 3D morphing based on geometrically constrained sphere mapping optimization. In: Proceedings of 2010 ACM Symposium on Applied Computing, pp. 1258–1265. ACM (2010)
2. Dehne, F.: Algorithms and Data Structures: Third Workshop, Montreal, Canada, 11–13 August 1993, WADS 1993. LNCS, vol. 709. Springer, Heidelberg (1993)
3. Hu, J., Zou, G.J., Hua, J.: Volume-preserving mapping and registration for collective data visualization. IEEE Trans. Vis. Comput. Graph. **20**(12), 2664–2673 (2014)

4. Lam, K.C., Gu, X., Lui, L.M.: Genus-one surface registration via Teichmüller extremal mapping. In: Golland, P., Hata, N., Barillot, C., Hornegger, J., Howe, R. (eds.) MICCAI 2014. LNCS, vol. 8675, pp. 25–32. Springer, Heidelberg (2014). doi:10.1007/978-3-319-10443-0_4
5. Li, X., Xu, H., Wan, S., Yin, Z., Yu, W.: Feature-aligned harmonic volumetric mapping using MFS. Comput. Graph. **34**(3), 242–251 (2010)
6. Miyauchi, S., Morooka, K., Tsuji, T., Miyagi, Y., Fukuda, T., Kurazume, R.: Area- and angle-preserving parameterization for vertebra surface mesh. In: Yao, J., Glocker, B., Klinder, T., Li, S. (eds.) Recent Advances in Computational Methods and Clinical Applications for Spine Imaging. LNCVB, vol. 20, pp. 187–198. Springer, Heidelberg (2015). doi:10.1007/978-3-319-14148-0_16
7. Miyauchi, S., Morooka, K., Miyagi, Y., Fukuda, T., Tsuji, T., Kurazume, R.: Tissue surface model mapping onto arbitrary target surface based on self-organizing deformable model. In: 2013 Fourth International Conference on Emerging Security Technologies (EST), pp. 79–82. IEEE (2013)
8. Miyauchi, S., Morooka, K., Tsuji, T., Miyagi, Y., Fukuda, T., Kurazume, R.: Angle- and volume-preserving mapping based on modified self-organizing deformable model. In: 23rd International Conference on Pattern Recognition (2016)
9. Miyauchi, S., Morooka, K., Tsuji, T., Miyagi, Y., Fukuda, T., Kurazume, R.: A method for mapping tissue volume model onto target volume using volumetric self-organizing deformable model. In: SPIE Medical Imaging, p. 97842Z. International Society for Optics and Photonics (2016)
10. Morooka, K., Nagahashi, H.: Self-organizing deformable model: a new method for fitting mesh model to given object surface. In: Bebis, G., Boyle, R., Koracin, D., Parvin, B. (eds.) ISVC 2005. LNCS, vol. 3804, pp. 151–158. Springer, Heidelberg (2005). doi:10.1007/11595755_19
11. Sederberg, T.W., Parry, S.R.: Free-from deformation of solid geometric models. Proc. ACM SIGGRAPH Comput. Graph. **20**(4), 151–160 (1986)
12. Shi, R., Zeng, W., Su, Z., Damasio, H., Lu, Z., Wang, Y., Yau, S.T., Gu, X.: Hyperbolic harmonic mapping for constrained brain surface registration. In: Proceedings of IEEE Conference on Computer Vision and Pattern Recognition, pp. 2531–2538 (2013)